







Article

## Meteorological Observations of the Vento Norte Phenomenon in the Central Region of Rio Grande do Sul

Cinara Ewerling da Rosa<sup>1,2</sup> , Michel Stefanello<sup>2</sup> , Ernani de Lima Nascimento<sup>2</sup> ,  
Fábio Diniz Rossi<sup>3</sup> , Debora Regina Roberti<sup>2</sup> , Gervásio Annes Degrazia<sup>2</sup> 

<sup>1</sup>*Instituto Federal Farroupilha, Campus Farroupilha, São Vicente do Sul, RS, Brasil.*

<sup>2</sup>*Departamento de Física, Universidade Federal de Santa Maria, Santa Maria, RS, Brasil.*

<sup>3</sup>*Instituto Federal Farroupilha, Campus Alegrete, Alegrete, RS, Brasil.*

Received: 13 November 2020 - Accepted: 6 April 2021

### Abstract

During the cold season, episodes of a windstorm known as Vento Norte (VNOR) are frequently observed in the city of Santa Maria, situated in the central region of Rio Grande do Sul (RS). The onset of this windstorm is characterized by strong gusts with northerly component which are accompanied by a sharp increase in temperature and abrupt drying. A methodology based on the observed behavior of the standard deviation of temperature during VNOR was successful in identifying the onset and demise of the windstorm. Additionally, the research shows the results of different micrometeorological variables during the event. Early morning and evening atmospheric profiles exhibit an elevated mixed layer over central RS in association with the strong VNOR winds, indicating the presence of mechanically-forced mixing during nighttime hours.

**Keywords:** Vento Norte, turbulence, windstorm.

## Observações Meteorológicas do Fenômeno Vento Norte na Região Central do Rio Grande do Sul

### Resumo

Durante a estação fria, episódios de uma ventania conhecida como Vento Norte (VNOR) são frequentes na região central do Rio Grande do Sul (RS). O fenômeno é caracterizado por intensas rajadas de vento de direção norte, acompanhadas de um aumento abrupto de temperatura e acentuado secamento. O estudo aponta que uma metodologia, baseada nas observações do desvio padrão de temperatura, permite identificar o início e término do fenômeno. Adicionalmente, o estudo mostra resultados de diferentes variáveis micrometeorológicas durante a ocorrência do evento. Perfis atmosféricos de início da manhã e de início da noite exibem uma camada mistura elevada sobre o centro do RS em associação com os fortes ventos do VNOR, indicando a presença de mistura turbulenta forçada mecanicamente durante o período noturno.

**Palavras-chave:** Vento Norte, turbulência, ventania.

### 1. Introduction

Understanding the characteristic scales of motion present in the Planetary Boundary Layer (PBL) and their interactions with larger-scale phenomena is crucial for the correct description of the transport of scalar and vector quantities occurring between the surface and the atmosphere. The study of wind characteristics, such as intensity, direction, duration, and other patterns, is essential in

investigating these transport processes (Kaimal and Finnigan, 1994). As such, turbulence produced by the wind field is an important process that must be adequately parameterized in weather and climate numerical models.

Among the wind systems that can alter the regular diurnal cycle of turbulence and temperature in the PBL, are the topographically-induced circulations. Under some circumstances such winds can become particularly

intense, especially on the downslope side of elevated terrain features (Decker and Robinson, 2011; Karmosky, 2019; Elvidge and Renfrew, 2016; Durran, 2015; Whiteman, 2000). These wind systems, or windstorms, disturb the local conditions in such a way that induce anomalies in the atmospheric variables that can depart significantly from the regional climatology for a given time of the year and/or time of the day (Elvidge and Renfrew, 2016; Math, 1934; Brinkmann, 1971; Norte, 2015; Raphael, 2003; Mass and Ovens, 2019; Smith *et al.*, 2018, Liu *et al.*, 2020). In general, with the downslope windstorms, high temperatures and very dry conditions are observed (Sartori, 2003). These phenomena can last for several hours and even days, and are known for the hazards that accompany them, such as thermal discomfort, damage to residential roofs, natural fires, reduced animal and plant production, among others (Sartori, 2003).

During the cold season, occasional episodes of moderate to strong northerly winds are observed around the city of Santa Maria, located in the central depression of Rio Grande do Sul state (RS), in southern Brazil. These winds, that develop under pre-frontal environments, are known as “Vento Norte” (VNOR; Sartori, 2003; Anabor *et al.*, 2005; Chamis and Nascimento, 2012; Stefanello *et al.*, 2020). The VNOR is characterized by intense gusty winds accompanied by unseasonably high temperatures and drop in the dew points, and it affects the turbulence behavior in the PBL, impacting the transport and diffusion of scalar and vector species and evapotranspiration (Arbage *et al.*, 2008). Furthermore, the strongest episodes of VNOR affect local essential activities such as agriculture (Heldwein *et al.*, 2003).

In addition to the synoptic-scale forcing, there is strong evidence that effects associated with the local topography in the central region of RS enhance the VNOR winds in Santa Maria and vicinities (Sartori, 2003; Stefanello *et al.*, 2020; Sartori, 2016). Despite being an important regional weather system for RS state, the characteristics of the VNOR phenomenon have been little studied and documented (Sartori, 2003; Anabor *et al.*, 2005; Stefanello *et al.*, 2020; Arbage *et al.*, 2008; Sartori, 2016; Nascimento, 2018).

The main goal of this work is to describe some micrometeorological characteristics of a prolonged VNOR event as sampled by a micrometeorological tower installed in Santa Maria's. This event was selected from a number of VNOR episodes that occurred in 2018 and that were identified by the application of a set of criteria for VNOR detection on the hourly data made available by Santa Maria automated surface weather station operated by the National Institute of Meteorology (INMET). Building upon the micrometeorological analysis, a secondary goal is to identify dynamic parameters that indicate the onset and demise of the VNOR. Additionally, an analysis is conducted of the vertical profiles sampled by operational

soundings from Santa Maria Air Force Base (SBSM) before, during, and after the VNOR event.

The paper is organized as follows. Section 2 presents an overview of the detection of episodes as well as the turbulence parameters applied to the study. Section 3 offers a discussion of a VNOR case study based on dynamic, thermodynamic, and atmospheric profiles. An investigation of the behavior is carried out, classifying the onset and demise of the phenomenon.

## 2. Material and Methods

For the characterization of the VNOR event, data from the winter months of 2018 were used, measured by a sonic anemometer (IRGASON-Campbell Scientific), installed in a micrometeorological tower at 3 m high at a frequency of 10 Hz. The tower is located in an area of the Pampa ecosystem within the campus of the Federal University of Santa Maria (29.72° S, 53.76° W; elevation of 88 m), as illustrated in Fig. 1 (Roberti *et al.*, 2012).

In this study, the criteria that characterize the occurrence of an VNOR event have been modified concerning that suggested in (Chamis and Nascimento, 2012) which were based on hourly data from the automatic station of



**Figure 1** - Micrometeorological tower installed at the Santa Maria experimental site. Photography: personal collection of researcher Michel Stefanello (2017).

the INMET located in Santa Maria at 10 m in height (29.72° S, 53.72° W; elevation 103 m). The criteria used here are:

- Wind: North quadrant direction, varying between 300° (West-Northwest) and 30° (North-Northeast);
- Wind speed: average above 4 m.s<sup>-1</sup> during the period in which the wind direction is within the direction criteria presented above;
- Surface air temperature: measured above the 90th percentile of the respective time and month;
- Duration: minimum of four consecutive hours.

From these preliminary criteria, the cases of VNOR were then identified. In this situation, the magnitude of the average velocity of 4 m.s<sup>-1</sup> was a criterion used to identify potential events for VNOR. It is important to note that this magnitude of the wind is small to be considered a windstorm. However, during episodes of VNOR the gusts of wind, which overlap this average value (mean wind speed in 3 s, not analyzed in this study) are typically above 10 m.s<sup>-1</sup>, with extreme cases exceeding 25 m.s<sup>-1</sup> (Sartori, 2003; Chamis and Nascimento, 2012).

The procedure for identifying the events of VNOR was carried out for the winter of 2018 in Santa Maria using data from the micrometeorological tower. The episode that took place between 19 and 20 July 2018 was chosen for the study. The longest in the winter, this event lasted 22 h and 25 min, which allows a detailed analysis of the turbulent flow during the windstorm to be performed in a complete daytime cycle.

The evolution of meteorological variables and turbulent parameters was determined using a time window of 5 min. The eddy covariance technique was used to characterize the surface turbulence structure and the friction velocity ( $u_*$ ). The friction velocity is defined mathematically by the following expression (Panofsky and Dutton, 1984):

$$u_* = \left( \overline{w'u'}^2 + \overline{w'v'}^2 \right)^{1/4}$$

where  $\overline{w'u'}$  and  $\overline{w'v'}$  define the turbulent momentum flux in the direction of the  $u$  and  $v$  components of the wind vector, respectively.

The sensible heat flux is defined by:

$$H = \rho C_p \overline{w'T'}$$

where  $\rho$  represents the density of the air,  $C_p$  the specific heat of the air at constant pressure, and  $\overline{w'T'}$  the covariance between temperature and vertical velocity component.

The kinetic energy of the turbulence was calculated using the following equation:

$$TKE = \frac{1}{2} (\sigma_u^2 + \sigma_v^2 + \sigma_w^2)$$

where  $\sigma_u$ ,  $\sigma_v$ ,  $\sigma_w$  are the standard deviations of the components  $u$ ,  $v$  and  $w$  of the wind velocity.

Upper air data from 00 UTC and 12 UTC operational soundings conducted at SBSM (29.71° S, 53.69° W; elevation 85 m) during the VNOR episode were also analyzed to characterize the prevailing atmospheric conditions in terms of stability and wind profile. The Sounding and Hodograph Analysis and Research Program in Python (SHARPPy; Blumberg *et al.*, 2017) package was used to produce the thermodynamic diagrams for the soundings.

### 3. Results and discussion

#### 3.1. Dynamic and thermodynamic analysis during VNOR

Figure 2 shows the temporal evolution of meteorological variables during the prolonged episode of VNOR. The average wind speed ( $U$ ) (Fig. 2a) increases significantly around 09:00 LST (Local Standard Time = UTC - 3 h) at the onset of the VNOR event. The average wind speed magnitudes remain high, with the highest values around 6 m.s<sup>-1</sup> occurring between 10:00 and 14:00 LST. As a comparison, in the study by Arbage *et al.* (2008), using data measured in a micrometeorological tower installed in Paraíso do Sul (29.74° S, 53.14° W) speeds of 7 m.s<sup>-1</sup> were observed. In the period between 17:30 and 22:30 LST of the first day, the wind speed decreased ( $U \sim 3$  m.s<sup>-1</sup>), however, this value is still high when compared to the average ( $U \sim 1.5$  m.s<sup>-1</sup>) observed in the morning preceding the episode of VNOR (02:00 to 09:00 LST).

The second meteorological variable analyzed is the temperature ( $T$ ), shown in Fig. 2b. This Figure makes it possible to identify an abrupt increase in temperature on the first day of the VNOR episode, occurring at 09:00 LST and exceeding the 90th percentile of the month 08:25 LST. This sharp increase in temperature coincides with the magnitude's intensification and the change in the wind direction (Fig. 2c). In this respect, it can be seen that at 09:00 LST on July 19, 2018, the wind acquires a vital North component, slightly inclined in the North-Northwest quadrant (meteorological angle of 343°) that remains in this until 07:30 LST on July 20, 2018.

Even in the winter period, the temperature, which local average is 13.4 °C (Climate Standards-INMET), exceeds 30 °C. Therefore, the daily temperature cycle is disturbed by the establishment and consolidation of air-flow, originating from the North direction, with temperature values remaining almost constant and high for the event entire period. At the end of the prolonged VNOR event, there is a noticeable drop in temperature, on the order of 9 °C, at 08:00 LST, falling below the 90th percentile after 08:15 LST. Likewise, there is a marked variation in the direction of the wind in the West-Southwest direction.

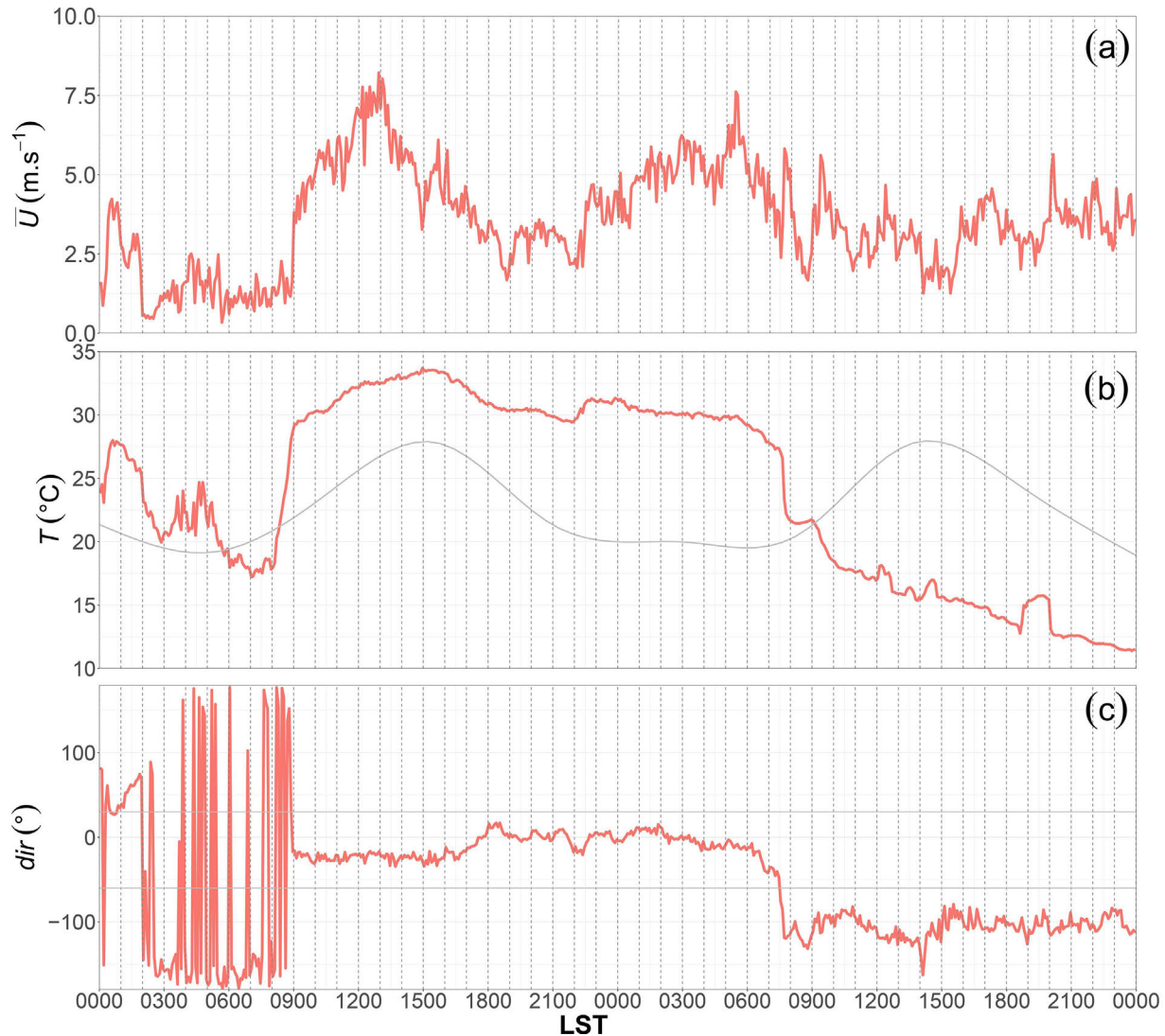


**Figure 2** - Average time series of 5 min for the VNOR event, from 19 to 20 July 2018. (a) average wind speed, (b) temperature and 90th percentile [gray], and (c) wind direction.

Additionally, as shown in Fig. 3, the predominant wind direction during the VNOR is fixed within the West-Northwest quadrant, oscillating around the average of  $349^{\circ}$ . The most intensity of the wind occurs in the Northwest direction ( $315^{\circ}$  and  $345^{\circ}$ ), while the highest frequency is in the North direction ( $345^{\circ}$  and  $15^{\circ}$ ). This flow pattern is different from that which usually occurs in the winter period.

Intense fluctuations in turbulent speed characterize the VNOR phenomenon. This characteristic encourages the observation and investigation of different turbulent statistical parameters associated with this natural flow pattern. This information on the VNOR turbulence can be used in pollutant dispersion models, in the generation of wind energy, and in crops (Heldwein *et al.*, 2003). The turbulent statistical parameters associate a episode VNOR are shown in Fig. 4. Figure 4a, shows the variance of the

vertical wind component ( $\sigma_w^2$ ). This magnitude demonstrates an intensification of turbulent activity. In this case, the high average values are in the order of  $0.5 \text{ m.s}^{-1}$ . The highest values of  $\sigma_w^2$  are around  $0.6 \text{ m.s}^{-1}$ , which occur in the initial period of the phenomenon 08:50 to 12:00 LST.

Figure 4b, shows the standard deviation of the temperature ( $\sigma_T$ ). This statistical quantity has an extended period (between the peaks at 08:45 LST of July 19, 2018 and 07:40 LST of July 20, 2018) with low rates of variability ( $\sigma_T < 0.5 \text{ }^{\circ}\text{C}$ ). The following reason can explain the low variability of  $\sigma_T$ : the prolonged event of air advection with high temperature (practically constant) and significant speeds does not allow strong fluctuations to occur in this scalar quantity. Analyzing the behavior of  $\sigma_T$ , it can be seen that this statistical quantity clearly and objectively marks the onset and demise of the VNOR. This result follows the analysis carried out by Stefanello *et al.* (2020).

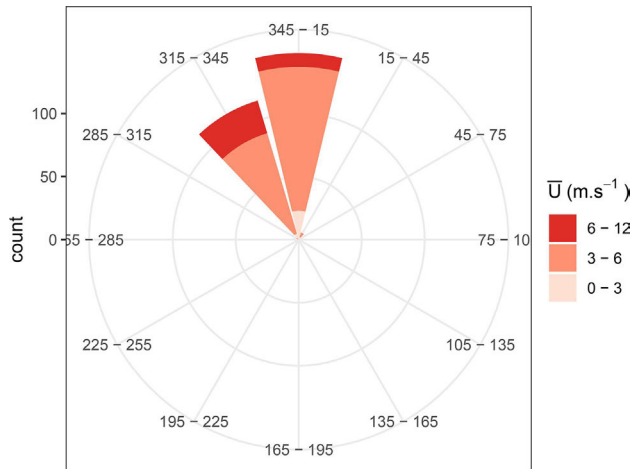


**Figure 3** - Compass rose for an extended event of VNOR, from 08:50 LST from July 19, 2018 to 07:25 LST from July 20, 2018.

These authors, investigating a case of VNOR, found that  $\sigma_T$  is an indicator that can be chosen to determine the onset and demise of an episode VNOR.

Large fluctuations at night, before detecting VNOR can be seen in the standard deviation of temperature. This period is characterized by the presence of low magnitudes of wind speed. It is possible to speculate that such values of  $\sigma_T$  are possibly associated with the downward propagation of the flow, which tends to disturb the stable boundary layer (SBL) located near the surface (Stefanello *et al.*, 2020). An attempt is made to reconcile the higher levels of the PBL with the surface.

Figure 4c shows the turbulent kinetic energy (TKE). It is noticed the growth of the production of turbulent mechanical energy during the phenomenon. Therefore, the ability to mix vector and scalar species during the event is very significant. In this case, the average value of  $1.2 \text{ m}^2 \cdot \text{s}^{-2}$  is well above the observed standard of  $0.24 \text{ m}^2 \cdot \text{s}^{-2}$  (average value for July 2018). An important velocity scale of the Surface Boundary Layer is the friction velocity ( $u_*$ ). Fig. 4d shows that this velocity scale follows the turbulent kinetic energy. During the event,  $u_*$  grows substantially, reaching an average value of  $0.5 \text{ m} \cdot \text{s}^{-1}$ . According to Garratt (1994), this value is a characteristic of the Neutral Boundary Layer. Therefore, it can be seen that the VNOR substantially disturbs the turbulent structure of the PBL.

Figure 4e shows the time evolution of the sensible heat flux ( $H$ ). On the first day of the VNOR, the  $H$  shows a peak at midday. Typically, this peak occurs at midday, in a Convective Boundary Layer (Stull, 1988). It can be seen from the figure that the positive  $H$  is shorter than typically observed (Stull, 1988). Therefore, in the presence of VNOR, the cooling of the PBL during the day is caused by mechanical turbulence (Arbage *et al.*, 2008).

Note that this sensible heat flux decreases in the afternoon and becomes negative well before sunset. From

the physical point of view, this behavior of the negative sensible heat flux, occurring well before the day-night transition, can be explained by the strong advection of warm air. In regions above the surface, the high air temperature, due to the effect of turbulence, tends to decrease the sensible heat flux caused by the high temperature of the air next to the ground.

From the discussion above, the turbulent statistical parameters, through their main characteristics, indicate the phenomenon period of occurrence. However, the strong effect on the variable  $\sigma_T$  (Fig. 4b) selects this parameter as a clear indicator of the onset and demise of the VNOR phenomenon.

Figures 2 to 4 show that the onset and demise of the prolonged VNOR event are strongly marked by evident variations in meteorological and micrometeorological variables. At 08:50 LST on the first day of the event, it is possible to observe a significant increase in speed in the predominant North/Northeast direction and increase surface temperature. These characteristics suggest that this is the onset of the phenomenon. The observed pattern is under the same phenomenon studied by Chamis and Nascimento (2012), which indicates that 70% of the episodes of VNOR start in the period from 00:00 to 10:00 LST. Such occurrence behavior can be linked to stability conditions (Chamis and Nascimento, 2012). On the other hand, these characteristics disappear at 07:25 LST on the second day of the event and mark the phenomenon's end.

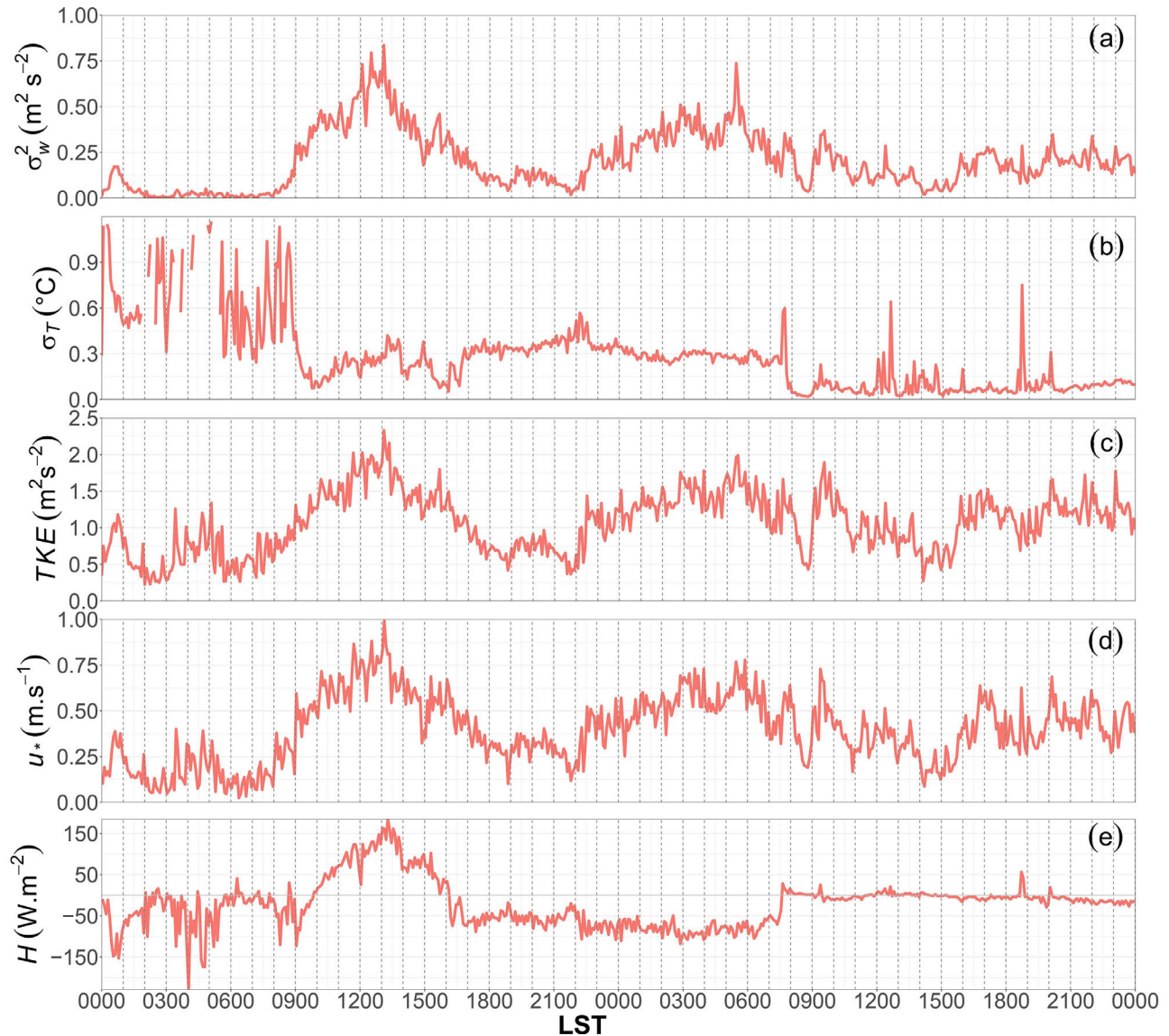
Figure 5 shows the relationship between the horizontal components of the wind (not rotated) and the surface temperature for the initial and final period of the VNOR episode.

Figure 5a shows two distinct wind patterns. The first, which occurs before the arrival of the surface phenomenon, characterized by low magnitudes of wind (order of  $1.5 \text{ m} \cdot \text{s}^{-1}$ ) and air with a temperature below  $20 \text{ }^\circ\text{C}$ . The second moment, which shows the onset of the episode of VNOR, identified by higher temperatures and higher wind speed. This transition between the two patterns occurs in short periods in which the temperature changed markedly.

The end of the VNOR event is represented in Fig. 5b. This end occurs after 22 h and 25 min from its onset and is marked by a smoother transition, when compared to its onset, presenting a decrease in temperature of approximately  $7 \text{ }^\circ\text{C}$ , with the wind components decreasing in magnitude, in less than an hour.

### 3.2. Atmospheric profiles over Santa Maria-RS during VNOR

Additional information regarding the VNOR event is obtained from the atmospheric profiles observed over Santa Maria-RS. The twice-daily operational soundings carried out between 00 UTC (21:00 LST) on July 18, 2018 and 12 UTC (09:00 LST) on July 20, 2018, at SBSM are shown in Figs. 6 and 7.



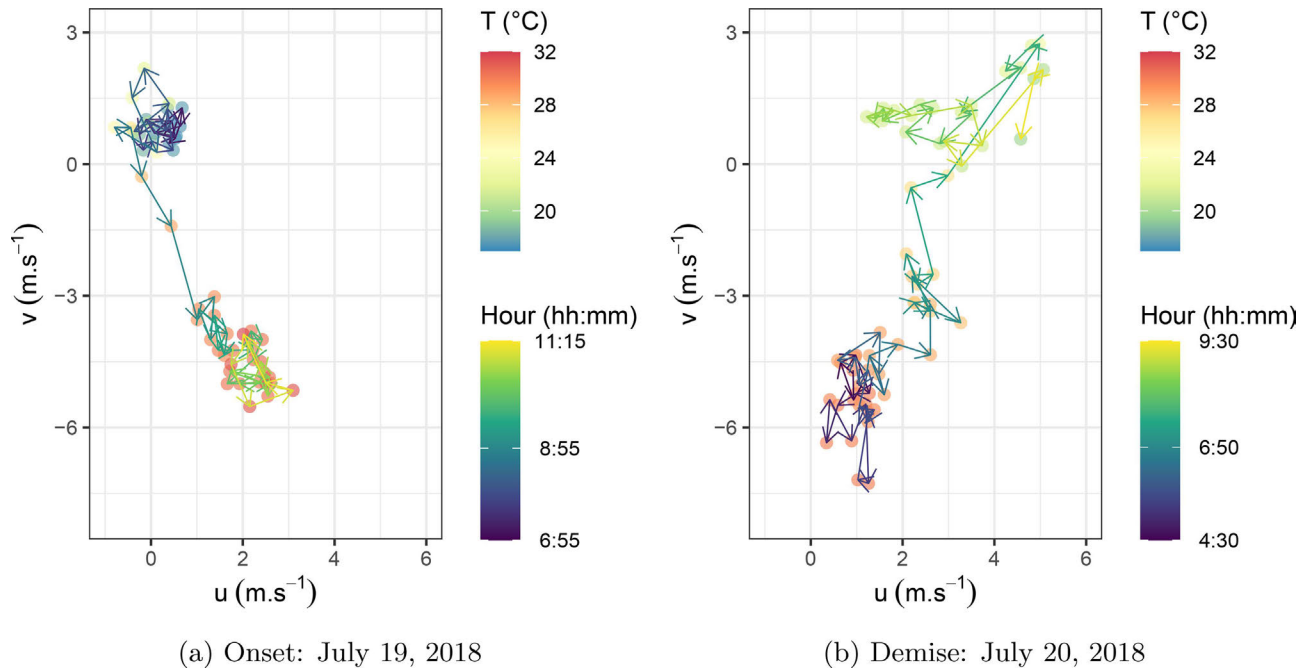
**Figure 4** - Average time series of 5 min for the prolonged VNOR event in the city of Santa Maria/RS, during the period from 19 to 20 July 2018. (a) variance of the vertical component of the wind, (b) standard deviation of the temperature, (c) turbulent kinetic energy, (d) friction velocity, (e) sensible heat flux.

Figure 6a shows the atmospheric profile hours before the start of VNOR. A dry air mass is in place, but with near saturation conditions at the surface, under a thermal inversion. Moreover, weak to calm surface winds suggesting that the formation of nighttime radiative fog was imminent (albeit not confirmed by the corresponding SBSM METAR reports).

The same sounding exhibits northerly winds promoting warm but dry advection at the top of the thermal inversion, located around 900 hPa. It is relevant to mention that Santa Maria is located in a depression, just south of an escarpment with a fairly abrupt 300 m drop in altitude. The moisture supply for the near fog conditions was limited to a very shallow surface-based layer below 300 m

(i.e., dammed in the depression), not affected by the moderately strong northerly winds just above, blowing from the elevated terrain. Immediately above the thermal inversion, a layer displaying significant mixing (i.e., a lapse rate very close to the dry-adiabat, and near-constant water vapor mixing ratio) extended up to about 750 hPa, characterizing, approximately, an elevated mixed layer (EML). This feature indicates that the northerly winds overrunning the stable nocturnal PBL over Santa Maria promoted mechanically-induced turbulence aloft, in a fashion similar to that described in Stensrud (1993).

The sounding launched in the morning (09:00 LST) of the following day (Fig. 6b), reported a surface temperature of 22 °C, which is much lower than the temperature



**Figure 5** - The initial and final path of VNOR event about horizontal wind and temperature components.

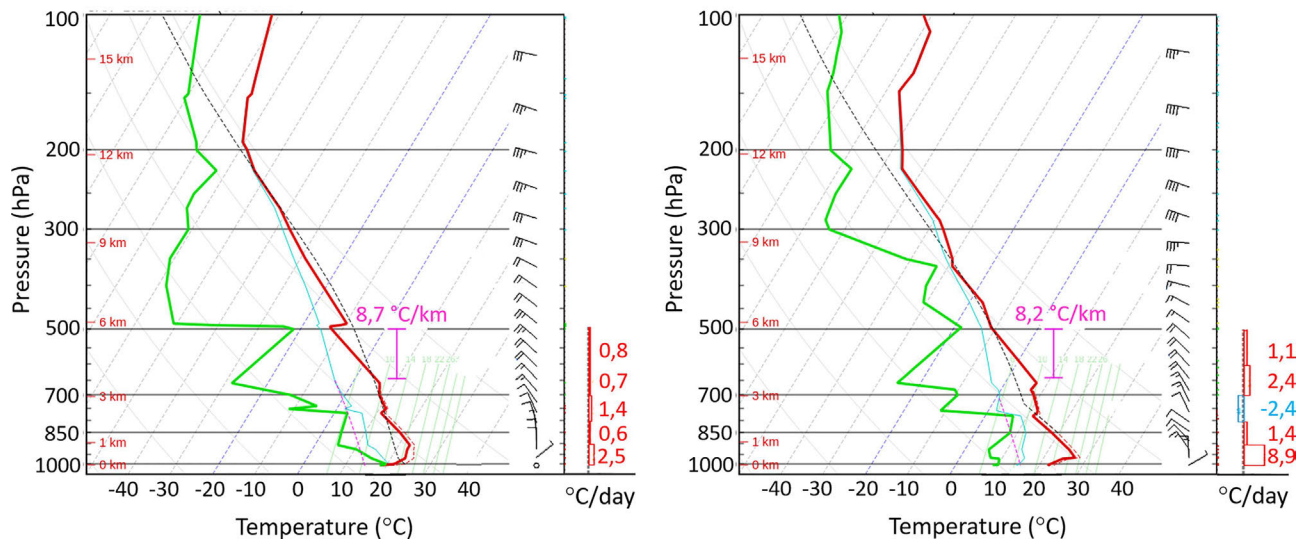


**Figure 6** - Skew-T diagrams of atmospheric soundings from SBSM at (a) 21:00 LST on July 18, 2018 and (b) 09:00 LST on July 19, 2018. The profile of air temperature [dew point temperature] is indicated by the red [green] line; barbs indicate the wind in  $\text{m.s}^{-1}$ . The environmental lapse rate for the most unstable layer is also reported (in  $^{\circ}\text{C.km}^{-1}$ ), as well as the temperature advection inferred from the vertical wind shear for five consecutive layers of 100 hPa depth from surface to 500 hPa, in  $^{\circ}\text{C.day}^{-1}$  (rectangles in the lower right corner of the diagrams)

reported at the same time by the micrometeorological tower. This discrepancy can be explained by the fact that the weather balloon is actually launched tens of minutes before 09:00 LST. This lag can also explain the surface winds of about  $5 \text{ m.s}^{-1}$  from east-northeast reported by the sounding, i.e., preceding the abrupt change in the wind direction observed close to 09:00 LST by the micrometeorological tower.

The same profile displays stronger northerly winds just above the surface, within the thermal inversion layer. At this time, the wind profile satisfied the definition of a low-level jet according to the criteria of Oliveira, *et al.* (2018). Compared to the previous sounding, the base of the EML is lower and the PBL is drier. It is interesting to notice that the EML, if extrapolated to the ground, would induce temperatures of about  $30 \text{ }^{\circ}\text{C}$  on the surface, con-

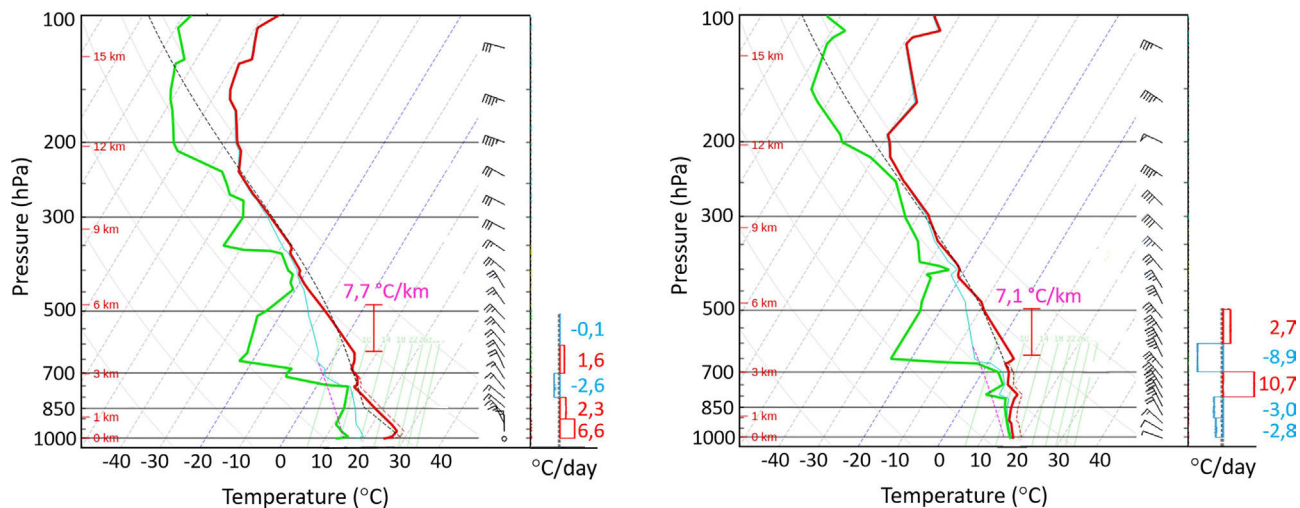


**Figure 7** - Skew-T diagrams of atmospheric soundings from SBSM at (a) 21:00 LST on July 19, 2018 and (b) 9:00 LST on July 20, 2018. The profile of air temperature [dew point temperature] is indicated by the red [green] line; barbs indicate the wind in  $\text{m}\cdot\text{s}^{-1}$ . The environmental lapse rate for the most unstable layer is also reported (in  $^{\circ}\text{C}\cdot\text{km}^{-1}$ ), as well as the temperature advection inferred from the vertical wind shear for five consecutive layers of 100 hPa depth from surface to 500 hPa, in  $^{\circ}\text{C}\cdot\text{day}^{-1}$  (rectangles in the lower right corner of the diagrams).

sistent with the temperature measured in the micrometeorological tower at 09:00 LST (Fig. 2b).

All these factors combined strongly suggest that the turbulence mechanically induced by the strong northerly winds in the EML was responsible for eroding the SBL from above throughout the early morning hours, until the warm and dry winds from north were finally detected at the surface, effectively characterizing the onset of the VNOR. This sequence of events is consistent with the presence of topographic features like the one in which Santa Maria is situated, comprising a sharp transition from a plateau to a depression perpendicular to the winds (e.g., Stensrud, 1993). Figure 6b also shows a significant intensification of the warm advection in the lowest layer, approaching  $9^{\circ}\text{C}\cdot\text{day}^{-1}$ .

The July 19th evening sounding (Fig. 7a) reveals the persistence of north and northwest winds in the lower troposphere and warm advection below 800 hPa. The layer between the surface and 850 hPa is warmer and drier than that observed 24 h before, because the base of the EML is closer to the surface. These aspects indicate a greater difficulty in establishing a nocturnal SBL in the presence of enhanced turbulence mechanically forced by the intense north winds. Still, a very shallow surface-based thermal inversion develops, and this is consistent with the weaker and more variable surface winds observed in the night hours when compared to the morning and afternoon hours of July 19th, 2018 (see Fig. 2a).

Finally, Fig. 7b shows the SBSM sounding valid at 09:00 LST of July 20th, 2018, a few hours after the demise of the VNOR, which occurred at 07:25 LST. The winds acquire a more intense westerly component in the layer from the surface to 850 hPa, and promote cold advection. The lower-tropospheric thermodynamic profile is also

substantially different from that observed in the previous sounding, with a drop in temperature and saturated, or near saturated, conditions. Although not a typical atmospheric profile of a frontal system, there is a clear change in air mass characteristics over Santa Maria at this time.

#### 4. Conclusions

In this paper, the turbulent characteristics of a prolonged episode of VNOR in July 2018 in the central region of RS were analyzed. The study employs high frequency (10 Hz) measurements of wind and temperature at an experimental site at the Federal University of Santa Maria.

The data analyzed in this study show that the average wind speed displayed magnitudes greater than  $4\text{ m}\cdot\text{s}^{-1}$  and direction varied between  $315^{\circ}$  at  $15^{\circ}$  during the VNOR episode. Temperatures surpassed  $28^{\circ}\text{C}$  during the entire event, with peak temperatures above  $32^{\circ}\text{C}$  in the afternoon hours, being substantially above the climatological average for July in Santa Maria ( $13.4^{\circ}\text{C}$ ; Climate Standards-INMET). The VNOR winds caused sharp changes in the magnitudes of the turbulent micrometeorological parameters. Quantities such as sensible heat flux, velocity variances, friction velocity, and TKE displayed robust magnitudes during the occurrence of VNOR for the day, mainly in the early morning and in the morning/afternoon transition. Therefore, the VNOR enhances the mixing of scalar and vector quantities in the PBL.

The standard deviation of temperature was the best micrometeorological indicator to define the onset and the demise of the VNOR phenomenon. A sharp and short-lived increase in this parameter was detected at the start of the VNOR, followed by a low standard deviation while



constantly high temperatures persisted during the event. At the end of the VNOR, another short-lived peak in the standard deviation was characterized, associated with the abrupt drop in temperature.

The atmospheric profiles sampled by the twice-daily operational soundings from SBSM also provided relevant information to understand the nature of the VNOR winds. Hours prior to the VNOR, a shallow nocturnal SBL, including weak winds and a surface-based thermal inversion, was in place in Santa Maria, with the surface being nearly saturated. The depth of the thermal inversion was comparable to the height of the terrain elevation situated just north of the city, suggesting the damming of colder air along the depression. Overrunning the SBL, warm and relatively strong northerly winds were observed, with an accompanying EML. Around the time of the VNOR onset, in the morning of July 18th, the northerly winds and the base of the EML were located much closer to the surface. This suggests that mechanically induced mixing coming from aloft was, to a large extent, responsible for the warming and drying of the PBL in Santa Maria, and that the onset of the VNOR event was associated with the mixing becoming recoupled to the surface. The EML persisted during the entire VNOR event, until low-level westerly winds associated with cold advection ended the VNOR winds. Additional studies involving high-resolution numerical simulations of actual VNOR events should address with more details the PBL evolution described above, including sensitivity to PBL parameterization schemes.

## Acknowledgments

This work was carried out with the support of the Federal Institute Farroupilha (IFFar), Graduate Program in Meteorology at the Federal University of Santa Maria (UFSM), and the Coordination for the Improvement of Higher Education Personnel - Brazil (CAPES) - Financing Code 001.

## References

- ANABOR, V.; ACEVEDO, O.; MORAES, O. Circulações termicamente induzidas na depressão central do Rio Grande do Sul. Parte I: intensificação noturna do Vento Norte. *Ciência & Natura* p. 391-395, 2005.
- ARBAGE, M.; DEGRAZIA, G.; WELTER, R.; ROBERTI, D.; ACEVEDO, O.; *et al.* Turbulent statistical characteristics associated to the North Wind phenomenon in southern Brazil with application to turbulent diffusion. *Physica A: Statistical Mechanics and its Applications*, v. 387, n. 16, p. 4376-4386, 2008.
- BLUMBERG, W.; HALBERT, T.; SUPINIE, P.; MARSH, R.; THOMPSON, J. Sharppy: An open-source sounding analysis toolkit for the atmospheric sciences. *Bulletin of the American Meteorological Society*, v. 98, n. 8, p. 1625-1636, 2017.
- BRINKMANN, W. What is a Foehn? *Weather*, Wiley Online Library, v. 26, n. 6, p. 230-240, 1971.
- CHAMIS, M.; NASCIMENTO, E. Condições atmosféricas associadas a episódios de “Vento Norte” na região central do RS. *Anais - XVII Congresso Brasileiro de Meteorologia*, 2012.
- DECKER, S.; ROBINSON, D. Unexpected high winds in northern new jersey: a downslope windstorm in modest topography. *Weather and forecasting*, v. 26, n. 6, p. 902-921, 2011.
- DURRAN, D. Mountain meteorology - Downslope winds. In: *Encyclopedia of Atmospheric Sciences* (Second Edition). Oxford: Academic Press, 2015.
- ELVIDGE, A.; RENFREW, I. The causes of foehn warming in the lee of mountains. *Bulletin of the American Meteorological Society*, v. 97, n. 3, p. 455-466, 2016.
- GARRATT, J. The atmospheric boundary layer. *Earth-Science Reviews*, v. 37, n. 1-2, p. 89-134, 1994.
- HELDWEIN, A.; STRECK, G.; BURIOL, M.; SANDRI, G.; TRENTIN, R.; *et al.* Frequência de ocorrência de ventos fortes em Santa Maria, RS. *Revista Brasileira de Agrometeorologia*, v. 11, n. 2, p. 285-291, 2003.
- KAIMAL, J.; FINNIGAN, J. *Atmospheric Boundary Layer Flows: Their Structure And Measurement*. Oxford University Press, 1994.
- KARMOSKY, C. Surface melt on ross ice shelf interior during a downsloping wind event. *Preprints*, 2019.
- LIU, Y.; DI, P.; CHEN, S.; CHEN, X.; FAN, J.; *et al.* Climatology of Diablo Winds in northern California and their relationships with large-scale climate variabilities. *Climate Dynamics*, p. 1-22, 2020.
- MASS, C.; OVENS, D. The northern California wildfires of 8-9 october 2017: The role of a major downslope wind event. *Bulletin of the American Meteorological Society*, v. 100, n. 2, p. 235-256, 2019.
- MATH, F. Battle of the Chinook wind at Havre, Mont. *Monthly Weather Review*, v. 62, n. 2, p. 54-57, 1934.
- NASCIMENTO, E. Ventanias com forçante topográfica no centro do Rio Grande do Sul: Estudo de caso do Vento Norte via modelagem numérica. *Anais - XX Congresso Brasileiro de Meteorologia*, p. 2367-2377, 2018.
- NORTE, F. Understanding and forecasting zonda wind (andean foehn) in argentina: a review. *Atmospheric and Climate Sciences*, 2015.
- OLIVEIRA, M.; NASCIMENTO, E.; KANNENBERG, C. A new look at the identification of low-level jets in south America. *Monthly Weather Review*, v. 146, n. 7, p. 2315-2334, 2018.
- PANOFSKY, H.; DUTTON, J. *Atmospheric Turbulence*. New York: Interscience, 1984.
- RAPHAEL, M. The Santa Ana winds of California. *Earth Interactions*, v. 7, n. 8, p. 1-13, 2003.
- ROBERTI, D.; ACEVEDO, O.; MORAES, O. A brazilian network of carbon flux stations. *Eos, Transactions American Geophysical Union*, Wiley Online Library, v. 93, n. 21, p. 203-203, 2012.
- SARTORI, M. Gênese e características do Vento Norte regional em Santa Maria/RS. *Anais - Simpósio Brasileiro de Geografia Física e Aplicada*, v. 10, 2003.

- SARTORI, M. **O Vento Norte**. Santa Maria: DR Publicidade Editora, ISBN: 978-85-66301-69-4, 2016.
- SMITH, C.; HATCHETT, B.; KAPLAN, M. A surface observation based climatology of Diablo-Like winds in California's wine country and western Sierra Nevada. **Fire**, v. 1, n. 2, p. 25, 2018.
- STEFANELLO, M.; NASCIMENTO, E.; ROSA, C.; DEGRAZIA, G.; MORTARINI, L.; *et al.* A micrometeorological analysis of the Vento Norte phenomenon in southern Brazil. **Boundary-Layer Meteorology**, Springer, v. 176, n. 3, p. 415-439, 2020.
- STENSRUD, D. Elevated residual layers and their influence on surface boundary-layer evolution. **Journal of Atmospheric Sciences**, v. 50, n. 14, p. 2284-2293, 1993.

- STULL, R. **An Introduction To Boundary Layer Meteorology**. London: Springer Science & Business Media, 1988.
- WHITEMAN, C. **Mountain Meteorology: Fundamentals And Applications**. Oxford: Oxford University Press, 2000.

### Internet Resources

Climate Standards-INMET, <https://portal.inmet.gov.br/normais>.

License information: This is an open-access article distributed under the terms of the Creative Commons Attribution License (type CC-BY), which permits unrestricted use, distribution and reproduction in any medium, provided the original article is properly cited.